
Article:
Koutas, L. orcid.org/0000-0002-7259-6910, Bousias, S.N. and Triantafillou, T.C. (2014) Seismic strengthening of masonry-infilled RC frames with TRM: Experimental study. Journal of Composites for Construction, 19 (2). 04014048. ISSN 1090-0268

https://doi.org/10.1061/(ASCE)CC.1943-5614.0000507

Seismic Strengthening of Masonry Infilled RC Frames with Textile-Reinforced Mortar: Experimental Study

L. Koutas[1]; S. N. Bousias, M. ASCE[2]; and T. C. Triantafillou, M. ASCE[3]

[1] Graduate student, Dept. of Civil Engrg., Univ. of Patras, Patras GR-26500, Greece. Email: koutasciv@upatras.gr
[2] Associate Professor, Dept. of Civil Engrg., Univ. of Patras, Patras GR-26500, Greece. Email: sbousias@upatras.gr
[3] Professor, Dept. of Civil Engrg., Univ. of Patras, Patras GR-26500, Greece. Email: ttriant@upatras.gr

Abstract:

The paper presents a technique for retrofitting non-seismically reinforced concrete (RC) masonry-infilled frames with textile-reinforced mortar (TRM) jacketing. In the present study the application of TRM is examined on nearly full-scale, as-built and retrofitted, three-storey frames, subjected to in-plane cyclic loading. The results of testing a 2:3 scale, as-built frame representing typical structures with non-seismic design and detailing characteristics and of a companion frame retrofitted via TRM jacketing are presented and compared in terms of the efficiency of the proposed technique to enhance the strength and deformation characteristics of sub-standard infilled frames.

Keywords: advanced composites; infilled frame; masonry infill; reinforced concrete; seismic retrofitting; strengthening; textile anchors; textile-reinforced mortar (TRM).

Introduction and Background

The effect of masonry infills over the entire response curve of existing reinforced concrete (RC) structures subjected to earthquake loading is significant, both before separation of the infill from the surrounding frame occurs – as encountered during frequent earthquakes – and during large cycles of imposed deformations near collapse. As reported in the literature, the most common beneficial contribution of the infills is the increase in, both, the global lateral stiffness and shear strength of infilled frames, and their contribution to the global energy dissipation capacity (e.g. Mehrabi et al. 1996, Fardis 1997). Nevertheless, the presence of infills induces or aggravates potential adverse effects, with the most critical one being the potential brittle shear failure of columns due to the additional shear demand in the column end-region where the, so-called, "diagonal strut" of the infilling is in contact with the frame members. In addition, regarding multistorey infilled RC buildings, there is a concern about the tendency for concentration of interstorey drift demand and damage within the 1st storey, ultimately leading to the development of a soft-storey mechanism (Fardis 2000). Strengthening of frame structures usually aims at increasing the resistance and deformation capacity of the frame itself, for the structure to comply with the code-prescribed levels of performance. A worth-examining alternative route to improve the performance of existing structures and avoid the excessive economic consequences of infill failure, is the effort of converting infilling to a more reliable source of resistance over the whole spectrum of structural response, through a guaranteed and quantifiable contribution to building's strength/stiffness. Several strengthening techniques have been proposed along this direction, with the application of sprayable ductile-fiber reinforced cementitious composites (e.g. Kyriakides and Billington 2008), and fiber-reinforced polymer (FRP) sheets (Ozcebe et al. 2003, Saatcioglu et al. 2005, Yuksel et al. 2006, Almusallam and Al-Salloum 2007, Altin et al. 2008, Akin et al. 2009, Ozden et al. 2011), being the most recent ones.

In the present study the very promising technique of application of textile-reinforced mortar (TRM) as externally bonded reinforcement, is for the first time employed to existing, masonry infilled, reinforced concrete frames. The effectiveness of this non-conventional, environmentally friendly material that combines advanced fibers, in the form of textiles, with inorganic matrices (e.g. cement-based mortars) for strengthening reinforced concrete structures has been reported less than a decade ago by Triantafillou et al. (2006), Triantafillou and Papanicolaou (2006) and Bournas et al. (2007); and more recently by D'Ambrisi and Focacci (2011), Al-Salloum et al. (2011, 2012) and Loreto et al. (2014). Tests on masonry sub-assemblies and wallettes have provided experimental evidence that TRM is effective in strengthening masonry structures too, as it enhances both the in-plane and out-of-plane strength (Papanicolaou et al. 2007, Papanicolaou et al. 2008, Harajli et al. 2010, Augenti et al. 2011, Papanicolaou et al. 2011, Babaeidarabad et al. 2013), as well as the strength in diagonal compression (Prota et al. 2006, Babaeidarabad et al. 2014). Nonetheless, in all these studies individual, single storey wall-type masonry specimens were employed, without considering the frame-wall interaction in multistorey structures.

The concept of TRM-strengthening masonry infilled RC frames has been described in the past by Koutas et al. (2014), who, as part of a broader experimental campaign, presented a first successful attempt to develop different infill-frame connection methods employing small-scale sub-assemblies. Key objective of the present study is the experimental investigation of the effectiveness of this new strengthening technique when employed in retrofitting multistorey, non-seismically designed masonry infilled frames.

Experimental Program

The single-storey, single-bay infilled frame test setup has been the configuration of preference in the majority of experimental studies investigating the response of infilled frames (either as-

built or after retrofitting), not only due to its simplicity but also because it facilitates the calibration of relevant numerical models. However, stress redistribution occurring in multistorey frames in which the load-bearing capacity of certain members is exceeded, cannot be represented by such test configuration. To draw conclusions on the response of actual systems, a 3-storey frame representing a full-height internal bay of an existing non-ductile building built in Southern Europe in the '60s, was considered in the present study. The test specimens comprise a 2:3 scale model of the prototype frame.

Test Specimens

Two identical infilled frames were designed and built: the first (Specimen #1) was tested as built and served as the control specimen, whereas the second (Specimen #2) was strengthened via TRM before been tested to failure. In addition to all parameters being kept identical between the two frames, construction of the infills by the same craftsmen and use of a common loading protocol, allow for the direct assessment of the effectiveness of the retrofitting method.

The geometry of the test frames is shown in Figure 1. For the 2:3 model-to-prototype scale selected, each storey resulted 2.0 m in height (3.0 m in the prototype) and 2.5 m between column centerlines (3.75 m in the prototype), yielding a length-to-height aspect ratio of 1.36 for the infill wall.

The columns were of rectangular cross-section 170x230 mm (with the long side parallel to the plane of the frame), whereas beams were of T-section, to account for the effective width of the slab (Fig. 2). The column longitudinal reinforcement consisted of deformed bars, lap-spliced only at the base of the first storey (connection to the foundation); a 60-bar-diameter splicing length was adopted to preclude splice failure prior to yielding of the longitudinal reinforcement. The transverse reinforcement for all concrete members consisted of plain bars with 90-deg hooks at the ends. As typical of sub-standard structures, the

thickness of the cover concrete to stirrups was low (10 mm). To represent the actual three-dimensional nature of column-beam joints, short transverse beams were constructed at all joints.

The average cylinder compressive strength of concrete on the day of testing for the foundation beam and each storey (average values from three specimens) was 27.8 MPa for Specimen #1 and 27.2 MPa for Specimen #2. The values of reinforcing steel yield stress were equal to 270 MPa and 550 MPa for the plain steel stirrups and for the rest (deformed) reinforcement, respectively.

Each 3-storey frame was cast in-situ in four stages, allowing for a 10-day period of construction and curing for each storey. The infills, which were constructed by perforated, fired clay bricks (185x85x55 mm) laid with the perforations running parallel to the unit's length, comprised two individual wythes separated by a 60 mm gap (Fig.3a). In total, the wall final thickness resulted equal to the width of the columns (170 mm). The 11.3 MPa mean compressive strength of the bricks perpendicular to the perforations was obtained as average of three tests on bricks capped with rapid-hardening sulfur mortar. The thickness of the bed and the head mortar joints was approximately 10 mm. The cement:lime:sand proportion in the mortar used to bind the bricks was 1:1:5. The flexural and compressive strength of the mortar was obtained according to EN-1015-11 (1993), as average of nine specimens. The compressive strength on the day of testing was 12.6 MPa (Specimen #1) and 13.3 MPa (Specimen #2), and the flexural strength was 2.6 MPa (Specimen #1) and 2.6 MPa (Specimen #2).

The construction of the masonry infilling commenced few weeks after completing the concrete frame and was implemented in two stages: all rows of masonry units in each bay were built, but the last one. The space left below the beam soffit was filled after a period of seven days, thus allowing for the development of substantial part of mortar shrinkage. To guarantee a minimum level of confinement to the masonry and represent the common practice

in the 60s, the last row of bricks was completed with the units being laid at slope (Fig.3b), pressing each one against the previous.

Strengthening Scheme

The selection of the strengthening scheme for Specimen #2 was dictated by the performance of the control specimen and was assisted by the results obtained from tests on small-scale specimens (Koutas et al. 2014) as well as by analytical calculations. In view of the shear failure of one of the columns of the as-built specimen (see results further on), the scheme for retrofitting Specimen #2 was based on the triptych: column strengthening to suppress the shear failure evidenced in the control specimen, strengthening of the infill walls via two-sided application of layers of TRM externally bonded on the faces of the infills, and provision for adequate anchorage of the TRM jacket around its perimeter via textile-based anchors and bond length.

In particular, the process for retrofitting Specimen #2 comprised the following steps:

- Strengthening the ends of columns at the first and second stories with three and two layers of TRM, respectively, fully wrapped around the member to form a closed jacket over a height of 420 mm (one-quarter of the clear column height). The number of layers of TRM was determined by the need to provide for column capacity in shear higher than the respective demand (obtained from Specimen #1). The need to guarantee the performance of the columns in shear opted for the solution of a fully closed jacket over the, easier to construct, open three-sided jacket, and despite the fact that in actual retrofitting projects a fully closed jacket would require partial demolition of the neighboring masonry. The fact that columns in non-ductile structures suffer a severe lack of shear resistance along with additional local distress at column ends induced by the infills, leads to the adoption of closed jackets as a more reliable strengthening approach for this case.

- Attachment of layers of TRM on both sides of the masonry infills, completely covering vertically the storey clear height (top of slab of lower storey to slab soffit of upper storey) and horizontally the area between the extremities of the bounding columns. The number of layers of TRM was determined on the basis of the response and damage observed in Specimen #1, as well as by analytical modeling of the infilled frame. As a result, the first storey received two layers of TRM, whereas the second and third storeys received one layer. Details on the exact sequence of application are provided subsequently.
- Insertion of textile-based anchors to provide composite action of the jacket at the slab-infill interfaces of the first and second storey, on both sides of the infill panels. In total 11 and 8 anchors per side were placed at equal spaces along these interfaces, at the 1st and 2nd storey, respectively. The corresponding spacing between the anchors was 200 mm and 300 mm for the 1st and 2nd storey, respectively. An extra textile patch was placed at the top frame-infill interface of the 1st and 2nd storey in order to enhance the interaction between the infill panel and the concrete beam at that level. These textile patches were placed on both sides of the second storey infill panel, but only on the back side of the first storey infill panel. On the top front side of the infill panel on the first storey the back-side patches were substituted by six 400 mm-spaced textile-based anchors, for the sake of comparison. Details on the anchors configuration are presented in Fig. 4.

The closed TRM jackets at the column ends of the first and second storey were based on a commercial carbon-fiber textile with equal quantity of fibers in two orthogonal directions. The mesh size and the weight of that textile were 10x10 mm and 348 g/m^2, respectively. For the application of the TRM layers on the faces of the infills a commercial polymer-coated E-glass textile (of 25x25 mm mesh size and 405 g/m^2 weight), also with equal quantity of fibers in two orthogonal directions, was used. The anchors used in this study were custom-made from a commercial textile made of uncoated basalt fiber rovings knitted in two orthogonal directions, with equal quantity of fibers in each direction. The mesh size and the weight of

that textile were 25x25 mm and 192 g/m^2, respectively. The properties of the textiles, either provided by the manufacturers or derived analytically (where full data are not available), are summarized in Table 1.

The mortar used as the binding material of the textile and the substrate was a commercial fiber-reinforced cement-based mortar (with water-to-cementitious material ratio equal to 0.22 by weight) mixed with re-dispersible polymers. Strength properties were obtained through flexural and compressive testing, as in the case of the mortar used for the construction of brick wallettes. The mean values of compressive and flexural strength (average values from 5 specimens) on the day of Specimen #2 testing were equal to 18.9 MPa and 4.3 MPa, respectively.

TRM was characterized through tension testing of coupons with dumbbell geometry (Fig. 5a). In total, twelve coupons were fabricated and tested after 28 days. Six of the coupons comprised one layer of glass fibers textile (see 2nd column of Table 1) while the rest six comprised two layers of the same textile. All TRM coupons were subjected to uniaxial tension, introduced by specially designed steel flanges fitting exactly the curved parts of the specimens (Fig. 5b). The behavior of all specimens was characterized by multiple cracking within the gauge length (Fig. 5c) and failure due to the rupture of fibers. From the obtained results, the tensile strength of TRM (average value from six specimens) was obtained: 47.6 kN/m and 78.7 kN/m for one and two textile layers, respectively. These values correspond to 41.4% and 34.2% of the tensile strength of the textile given by the manufacturer.

Details on the development of the textile-based anchors used in this study and the verification through testing can be found in Koutas et al. (2014). The anchors placed along the slab-infill interfaces on both sides of 1st and 2nd storey (denoted as W400-L350) were formed from a 400 mm-wide basalt textile sheet: a length of 100 mm of the textile was twisted to form a stub, while the rest 350 mm was opened to form a fan (Fig. 4). The series of anchors placed along the infill-slab soffit interface on only the front side of 1st storey (denoted as

W600-L500) were formed from a 600 mm-wide basalt textile sheet shaped in straight and fan-shaped parts of 100 mm and 500 mm, respectively. The angle of the fan was kept constant for all anchors and equal to 45^o (Fig. 4).

For the impregnation of the straight part of each anchor a commercial low viscosity, two-part epoxy resin adhesive was used during the anchor fabrication stage, with tensile strength and elastic modulus of 72.4 MPa and 3.2 GPa, respectively (as provided by the manufacturer). The adhesive used for impregnating the dry fibers in the central area of the anchors (a procedure employed during the strengthening stage) was a special type commercial, low viscosity, two-part epoxy resin, which can harden under high humidity conditions, as those encountered in the fresh mortar of the TRM system. The tensile strength and the elastic modulus of this adhesive were equal to 20 MPa and 3 GPa, respectively (as provided by the manufacturer).

Application of Strengthening Scheme

Strengthening of Specimen #2 was performed with the aid of experienced workers and is illustrated in Fig. 6. Strengthening the 1^{st} and 2^{nd} storey column ends with closed TRM-jackets preceded the infilling of the RC frame bays (Fig. 6b), to avoid demolishing the masonry infilling adjacent to the column ends. All concrete surfaces where mortar was to be applied were brushed clean and dampened. A thin layer of mortar was applied first on the dampened surfaces and then the textile sheet was wrapped by hand pressure around the chamfer-cornered column section (Fig. 7a). Mortar was applied in-between the layers of textile while the previous layer of mortar was in a fresh state, as well as on top of the last textile layer. The thickness of each layer was approximately 3 mm, yielding a closed jacket of approximate thickness of 9 mm and 6 mm for the 1^{st} and 2^{nd} storey, respectively.

Following the construction of the infills (Fig. 6c), the two-day long procedure for strengthening the infill panels commenced. Each of the six faces of the infills was

strengthened independently, following the same guidelines and the procedure described previously. In all cases, the first step was the application of the first TRM layer along both faces of the infill and around the bounding frame members (Fig. 6d, e). Due to its limited width (equal to 1500 mm), the textile was applied with an overlap of about 300 mm along the entire length of each bay, near the bottom part of each storey. The next step (involving only the 1st and 2nd storeys) comprised the application of the textile-based anchors and the extra textile patches in the corresponding regions (Fig. 6f). The straight parts of the anchors were inserted into pre-drilled 12 mm-diameter holes filled with injected epoxy resin, while the fanned parts were bonded by hand pressure on the top of the first TRM layer (Fig. 7b, c). The extra textile-patches were simply placed in the appropriate regions and bonded by pressure against the first TRM layer. Installation of the anchors was preceded by local impregnation of the dry fibers region with epoxy adhesive. The third step included the application of the second TRM layer on the faces of the 1st storey infill and the surrounding frame members (Fig. 6g, h). Here too, the textile was applied with an overlap of 300 mm, near the top part of each storey, so that the two overlapping regions would be located at different levels. The final step included wrapping of the overhanging textile parts around the chamfered corners of the column section and their bonding on the side faces of the columns (Fig. 6i).

The final thickness of the jacket on each side was equal to 12.5 mm and 7.5 mm for the 1st and 2nd/3rd storeys, respectively; these values are the average of several measurements at the mid- height of each storey. It is noted that in the regions of the 1st and 2nd storey columns ends, the total thickness of the externally bonded composite material was equal to 20 mm and 12.5 mm, respectively, including the TRM jacket thickness. Figure 8 presents a general view of Specimen #2 during different phases of retrofitting.

Test Setup and Procedure

Both specimens (control and retrofitted) were subjected to a sequence of quasi-static cycles of a predefined force pattern. A history of imposed cycles of displacements was defined to be applied at the top, while maintaining an inverted-triangular distribution of forces to all three floor levels until failure (in terms of global response) occurred. The displacement history of the 3rd storey is shown in Fig. 9. Except for an initial low-amplitude cycle of 1mm, a total of 5 and 7 cycles were finally applied to the unretrofitted and the retrofitted specimens, respectively. The number of cycles imposed on the two specimens was determined on the basis of achieving at least the conventionally defined failure threshold of 20% drop in the peak load.

A general view of the test set-up is shown in Fig. 10. Three servo-hydraulic actuators were mounted on the specimen, one per storey. The strong foundation beam was fixed to the laboratory strong floor via 16 prestressing rods to provide specimen full clamping. Special care was taken in order to exclude any out-of-plane specimen deformation resulting from eventual geometrical eccentricities. A system of 2 steel trusses with 2 transverse steel arms per storey was used to provide out-of-plane support to the specimen, leaving the in-plane behavior unaffected.

Gravity loading of 80 kN per storey was considered to represent the fraction of permanent loads concurrent to the lateral loading action. This load, mainly shared by the two columns of the frame, was realized through a set of 4 prestressing rods per storey. The use of different sets of prestressing bars per storey allowed heightwise non-uniform distribution of the axial load to be achieved, matching that obtained analytically (120 kN, 80 kN and 40 kN for the 1st, 2nd and 3rd storey, respectively). Thus, the varying confining conditions actually existing in each infill panel, as reported in Chrisafulli (1997), are represented effectively. In addition, the adopted configuration for the application of gravity loads respects the observations (Chrisafulli 1997) that in the lower stories of multistorey infilled frames the gravity loads are resisted mainly by the columns.

The instrumentation layout included:

- A network of 72 potentiometers at selected locations, monitoring: (a) the separation and sliding at the interfaces of the infills to the surrounding frame members, (b) the deformations of the diagonals of the infill panels, and (c) the deformation along 7 consecutive zones on the outer faces of the columns.
- A total of 24 strain gages, monitoring: (a) strains in the longitudinal reinforcement of 1st storey columns; 2 strain gages at 3 different levels along the height of each column, and (b) strains of the threaded bars used for applying the axial load in the columns.
- 3 highly accurate sensors (2 μm) to monitor/control the horizontal displacements at each storey level.

Experimental Results and Discussion

Specimen #1

The progressive cracking which developed in the 1st storey masonry panel of Specimen #1 is shown in Figure 11a, for 1st, 3rd and 5th cycles of loading. The first cracks developed already during the first cycle in the positive direction of loading, at a top displacement of approximately 6 mm (0.1% top drift ratio); two step-type cracks formed at the 1st storey, running in parallel to the diagonal, but not progressing much lower than the mid-height of the panel. This behavior is in agreement with the observation (Chrisafulli 1997) that if the horizontal projection of the length of a fully-developed step-cracking pattern is smaller than the horizontal dimension of the infill panel, then the step-type cracking forms away from the diagonal and is accompanied by horizontal sliding-type cracking (the latter was observed during the 3rd cycle in the present tests). The step-wise cracking pattern was observed in the direction of the opposite diagonal, after load reversal. Previously opened cracks re-opened, became wider and propagated in the body of the infill during the 2nd cycle of loading,

resulting in a marked decrease of the overall lateral stiffness of the frame. The cracking pattern was completed during the subsequent cycle with the formation of two sliding cracks, one at top of the infill (soffit of inclined bricks) and the other slightly lower than mid-height that joined the tips of the step-type cracks of the previous cycle. The maximum base shear force was attained during the 3rd cycle of loading; for the two directions of loading a maximum base shear of 264 kN/-252 kN was recorded at corresponding top displacement of 25 mm/-24 mm (1st storey drift ratio of 0.77%/-0.68%, Fig. 12b). During the same cycle the minor shear cracks that had opened at the top of both first storey columns became wider, especially at the top of the east-bound column. It is worth-mentioning that diagonal cracks in the 2nd storey infill panel appeared first during the 2nd cycle of loading, but their formation and evolution was not critical to the subsequent specimen performance.

The post-peak behavior of the specimen was non-symmetric (Fig. 12) with a rather softer descending branch of the envelope curve in the direction of positive loading (Fig.12a) compared to that of negative loading. For the positive direction of loading the post peak behavior reflects the progressive corner crushing failure of the strut in the 1st storey infill panel, due to high compressive stresses. In contrast, the post peak behavior in the opposite direction of loading reflects the shear failure at the top of the 1st storey east-bound column (shown in Fig. 13a), which occurred at an interstorey drift ratio as low as 0.7%. The test was intentionally terminated at the end of the 5th loading cycle. Figure 13b shows the damage in the masonry panel and at the top of the east-bound 1st storey column, upon test completion.

As mentioned earlier, separation of the infill from the surrounding frame members was monitored in the perimeter of the infill via a network of potentiometers. The general observations regarding the corresponding measurements are summarized below:

- Frame-infill separation occurred at the very early stages of loading; most of the sensors captured the opening of a gap even during the 1st cycle of loading (drift ratio 0.1%).
- The recordings of sensors in the 2nd/3rd storeys revealed infinitesimal frame-infill separation, with the size of the opening following the pattern of imposed cycles of loading. In contrast, recordings of relevant sensors at 1st storey deviate from that pattern, due to the presence of areas with high local deformations at the points of sensor attachment.
- The interfaces between the columns and the infill exhibited larger gap opening as compared to those at bottom slab-infill and top beam-infill interfaces, except for the bottom slab-infill interface of the 2nd and 3rd storey; in these cases the gap opening was of the same magnitude as the ones at the column-infill interfaces. The interfaces with practically zero gap opening were the bottom slab-infill interface of 1st storey, and the top beam-infill interfaces of 2nd and 3rd storey.
- The peak values of the measured gap opening were: (a) 2.0 mm for the 1st storey (at the column-infill panel interface), (b) 1.5 mm for the 2nd storey (at the bottom slab-infill panel interface), and (c) 0.7 mm for the 3rd storey (at the bottom slab-infill panel interface).
- Measurement of slippage along the top/bottom frame-infill interface showed the existence of considerable relative deformation which occurred either at exactly along the interface, or – as in the case of the beam soffit at both first and second storey – below the first row of inclined masonry units at the top of each panel.

Specimen #2

Compared to control Specimen #1, the retrofitted specimen (Specimen #2) exhibited initial cracking at essentially the same displacement level as in the control specimen (1st cycle); minor cracks appeared on the external face of the TRM jacket at the lower-left quarter of the 1st storey infill panel (Fig. 11b). Similar cracking was observed at the mirror region,

upon load reversal. During the subsequent cycles of loading a more dense - compared to Specimen #1 - cracking pattern developed, composed of inclined cracks (close to the corners of the infill panel) and of sliding-type cracks (mostly at the central region of the panel). Infill panel separation from columns and few cracks parallel to the diagonal developed on the 2nd storey infill panel (Fig. 14a, b) – this pattern remained unaltered for the rest of testing. No signs of distress of the infill panel of the 3rd storey were observed, except for a vertical crack separating the panel from the west-bound column.

The response of the retrofitted specimen in terms of lateral force-top displacement is compared in Fig. 12 to that of the control specimen. The maximum base shear force of +407 kN/-395 kN recorded in the former in the positive/negative direction of loading, respectively, constitutes a 56% increase over that of the unretrofitted specimen and was attained during the 4th cycle. The top storey displacement at the instance of maximum base shear was approximately 40 mm, corresponding to 0.67% top drift or ±1.0% 1st storey drift (Fig. 12). The gradually decreasing lateral strength that followed the 4th cycle was the result of two combined phenomena; complete debonding of the TRM from the beam surface on the back side of the 1st storey (Fig. 13c) and gradual disintegration of the 1st storey infill at the two upper ends neighboring the columns (local crushing). In the subsequent loading cycles, very large strains were induced in the TRM at these two corner regions on the back side of the specimen (the one without anchors at the top of the 1st storey), leading to rupture of fibers (Fig.13c). An important observation regarding the post peak-strength behavior of the specimen was that the anchors placed at the top of the front side-1st storey infill were actually activated and contributed in delaying the debonding of the TRM; debonding in this case occurred during the 6th cycle of loading and all six anchors fractured during the 7th cycle. The different behavior of the TRM between the top front and the top back sides of 1st storey clearly indicates that the extra textile placed at this region was not as effective as the provision of anchors. Nevertheless, the demand for improved anchoring conditions of the

TRM at the upper stories of the specimen was limited and the absence of anchors did not lead to debonding of the TRM. Regarding the anchorage of the TRM layers to the frame columns it was observed that debonding of the TRM only occurred at the mid-height of the 1st storey columns following the completion of the 5th loading cycle. At these regions the TRM layers were simply extended from the infill and bonded to the surface of the surrounding columns, whereas at the column end regions the textiles were turned around the column corner and proved effective to prevent debonding. At the upper stories no debonding of the TRM appeared along the interface to the columns. The anchors placed at the base of the 1st and 2nd storey infill panels did not exhibit any type of distress.

The TRM jackets which were applied at the ends of the 1st and 2nd storey columns successfully prevented pre-emptive shear failure of the type observed in the un-retrofitted specimen, while also providing the necessary confinement for the columns to go unscathed through high levels of drift. Figure 13d depicts the damage at the 1st storey after test completion.

Measurements from the sensors placed at the frame-infill interface to record eventual opening of the interface or relative slippage at the interface were not much different in the two specimens. They, however, definitely indicate that frame-infill separation was not avoided or eliminated after applying the textile layers and the response of the frame-infill system was far from monolithic.

Evaluation of the TRM strengthening technique

The application of the selected strengthening approach resulted in an improved response of the 3-storey masonry infilled RC frame. The improvement was not only achieved in terms of increased lateral resistance (reaching a 56% increased at peak resistance), but also in terms of stiffness. The lateral (secant) stiffness, as obtained for the 1st storey from the storey shear-

interstorey drift loops, is shown in Fig. 15 for different levels of the interstorey drift ratio. The retrofitted specimen displayed higher lateral stiffness compared to the control specimen, especially at the first storey and at low interstorey drift ratio (less than 0.5%). This is attributed to the presence of the layers of high strength cementitious mortar used as matrix for the textile – the layers were thicker than at the rest stories, as two layers of TRM were employed at the 1st storey. At the initial loading cycle in which the cementitious mortar was uncracked and the frame-infill-TRM system behaved as integral, the retrofitted specimen exhibited an almost twofold increase in stiffness compared to the as-built specimen. At increasing interstorey drift ratio the lateral stiffness is shown to degrade progressively in both specimens, almost following a hyperbola. The cementitious mortar could not sustain the large drift demands following the post-peak strength cycles, and thus failed in shear and disintegrated. The local failure of the mortar enabled the textile to deform independently from the masonry substrate (see Fig. 16 revealing the appreciable shear distortion of the textile at the region enclosed between two horizontal sliding interfaces) and a new load-transfer mechanism was formed in which the - free to distort - textile assumed the role of bridging the regions across a sliding interface. These localized phenomena at the retrofitting material level ultimately led to a slowly progressive degradation of strength and stiffness at the level of global response. This constitutes a further advantageous characteristic of the TRM system: the structural integrity of the textile is maintained, rendering it capable of containing the masonry infill and reducing the risk of out-of-plane collapse or of becoming dangerous to users. In this respect, the superior response of the anchors employed at the top front side of the 1st storey compared to detachment of the simple patch used in the respective area on the back side, cannot be overlooked.

The contribution of retrofitting in modifying the height-wise distribution of lateral deformation is shown in Fig. 17. While the response of the control specimen points more towards that of formation of soft-storey mechanism (due to the damage of one of the 1st storey

columns), lateral deformations in the retrofitted specimen are more evenly distributed along height, for at least up to 0.64% top drift ratio (4th cycle of loading). Nevertheless, in the post-peak region of response the strengthened specimen did not manage to retain the favourable distribution of lateral deformations and the ensuing damage of the masonry at the 1st storey led to increasing deformation demands at this level. This is evidenced in Fig. 18, showing the condition of the masonry at 1st storey after-test, in which not only a much more dispersed damage in the infilling of the retrofitted specimen is noted, but also inclined cracks at mid-height of 1st storey columns are revealed. This clearly indicates initiation of shear failure in the unretrofitted part of the columns owing to fracturing of the masonry regions in contact to the columns and points to the suggestion that, to avoid eventual shear failure after masonry has failed, columns should be strengthened in shear along their full height.

The progressive cracking of the cementitious mortar of the strengthening scheme and the eventual activation of the textile at higher levels of deformation provided for an effective dispersion of deformation demands over a broader area of the masonry infilling. Calculation of the cumulative hysteretic energy based on the base-shear versus top-storey displacement hysteretic loops (expressed by the area enclosed within the loops), shows that by the end of the 5th loading cycle (0.87% drift ratio) the retrofitted specimen had dissipated 22.5% more energy compared to the unretrofitted one. This reflects the contribution of the strengthening material in consuming energy, mainly due to the multi-cracking mechanism and the redistribution of the shear stresses on the body of the masonry infill. It should be noted that the capacity of a textile to distort in shear depends directly on its shear stiffness which, in the case of uncoated textiles, is practically zero and increases as the coating becomes heavier and the mesh size smaller (assuming the same stitching technique that was used for the fabrication of the textile). Hence, the geometry and the type of textile used for strengthening masonry infills should be considered as parameters necessitating further investigation.

A point to be addressed regarding the proposed strengthening technique is that the resulting increased base shear force (see Fig. 12a) imposes higher demands on the foundation system. In the present tests, the foundation element was dimensioned for the increased force/moment actions at the base; in actual applications, this issue will need to be particularly considered and the capacity of the foundation element should be verified against the expected increase in actions.

Conclusions

This paper presents an experimental study on the seismic retrofitting of nearly full-scale 3-storey masonry infilled frames employing non-conventional materials and techniques. The application of textile-reinforced mortar (TRM) as externally bonded reinforcement in combination with special anchorage details was examined on an as-built and a retrofitted 3-storey RC frame, subjected to in-plane loading. The results of testing a 2:3 scale, as-built frame representing typical non-seismically designed and detailed structures and of a companion frame retrofitted via TRM are presented and the efficiency of the proposed technique is discussed in detail. The main conclusions drawn are summarized as follows:

- The integrated retrofitting scheme resulted in an enhanced global response of the infilled frame both in terms of lateral strength and deformation capacity; an approximately 56% increase in the lateral strength was observed, accompanied with a 52% higher deformation capacity at the top of the structure at ultimate strength state. This point should receive the particular attention of designers, due to the increased moment that will need to be resisted by the foundation element and the strengthening this might imply.
- The retrofitted specimen dissipated 22.5% more energy compared to the control one, for the same loading history. The effect of retrofitting on the lateral stiffness of the 1st storey

is an almost twofold increase for low drift levels (up to 0.5%), becoming less pronounced at higher drift levels.

- The height-wise distribution of the lateral storey displacements was drastically modified in the retrofitted specimen, as column shear capacity enhancement by TRM wrapping supressed pre-emptive column shear failure caused in the control specimen by the lack of adequate transverse reinforcement and the concentration of high shear demands at column end regions induced by the so-called "diagonal strut".
- The application of TRM over the entire surface of infills should be supplemented with an adequate infill-frame connection, if a reliable resisting system is to be obtained. This conclusion is drawn, mainly, from the behavior of the TRM at regions beyond the frame-infill boundaries. The presence of custom-fabricated textile-based anchors was proved to be particularly effective in delaying or even precluding the debonding of TRM.
- Textile-reinforced mortar jacketing proved to be effective in withstanding large shear deformations through the development of a multi-crack pattern and by introducing an efficient load transferring mechanism at the local level. This mechanism is enabled by the capability of the textile itself to distort in shear, while retaining at the same time its structural integrity.

The present study is a first attempt to investigate TRM jacketing as a means of retrofitting infill walls in non-seismically reinforced, multi-storey concrete structures. Future research effort could be directed towards optimizing the materials in the TRM system and investigating out-of-plane loading effects.

Acknowledgements

This research has been co-financed by the European Union (European Social Fund – ESF) and Greek national funds through the Operational Program "Education and Lifelong Learning" of the National Strategic Reference Framework (NSRF) - Research Funding

Program HERACLEITUS II - Investing in knowledge society through the European Social Fund. The assistance of graduate student Anil Basnet and undergraduate students Eleni Pagoni, Giannis Triantafillou, Dimitris Tsitsokas and Stelios Kallioras in separate parts of the experimental program is also acknowledged.

References

Almusallam, T. H., and Al-Salloum, Y. A. (2007). "Behavior of FRP strengthened infill walls under in-plane seismic loading." *J. Comp. Constr.*, 11(3), 308-318.

Al-Salloum, Y. A., Siddiqui, N. A., Elsanadedy, H. M., Abadel, A. A., and Aqel, M. A. (2011). "Textile-reinforced mortar versus FRP as strengthening material for seismically deficient RC beam-column joints." *J. Compos. Constr.*, 15(6), 920-933.

Al-Salloum, Y. A., Elsanadedy, H. M., Alsayed, S. H., and Iqbal, R. A. (2012). "Experimental and numerical study for the shear strengthening of reinforced concrete beams using textile-reinforced mortar." *J. Compos. Constr.*, 16(1), 74-90.

Altin, S., Anil, Ö., Kara, E. M. and Kaya, M. (2008). "An experimental study on strengthening of masonry infilled RC frames using diagonal CFRP strips." *Composites: Part B*, 39(4), 680-693.

Akin, E., Ozcebe, G., and Ersoy, U. (2009). "Strengthening of brick infilled RC frames with CFRP sheets." *Seismic risk assessment and retrofitting with emphasis on existing low rise structures*, 367–386, A. Ilki, Karadogan. F., Pala S., Yuksel E., (eds.), Springer, Dordrecht.

Augenti, N., Parisi, F., Prota, A., and Manfredi, G. (2011). "In-plane lateral response of a full-scale masonry subassemblage with and without an inorganic matrix-grid strengthening system." *J. Compos. Constr.*, 15(4), 578-590.

Babaeidarabad, S., Caso, F., and Nanni, A. (2013). "Out-of-plane behavior of URM walls strengthened with fabric-reinforced cementitious matrix composite." *J. Compos. Constr.*, 10.1061/(ASCE)CC.1943-5614.0000457, 04013057.

Babaeidarabad, S., De Caso, F., and Nanni, A. (2014). "URM walls strengthened with fabric-reinforced cementitious matrix composite subjected to diagonal compression." *J. Comp. Constr.*, doi: 10.1061/(ASCE)CC.1943-5614.0000441.

Bournas, D., Lontou, P., Papanicolaou, C. G., and Triantafillou, T. C. (2007). "Textile-reinforced Mortar (TRM) versus FRP confinement in reinforced concrete columns." *ACI Struct. J.*, 104(6), 740-748.

Crisafulli, F. J. (1997). "Seismic Behavior of Reinforced Concrete Structures with Masonry Infills." PhD Dissertation, University of Canterbury, New Zeland.

D'Ambrisi, A., and Focacci, F. (2011). "Flexural strengthening of RC beams with cement-based composites." *J. Compos. Constr.*, 15(5), 707-720.

EN 1015-11 (1993). *Methods of test for mortar for masonry – Part 11: Determination of flexural and compressive strength of hardened mortar*, European Committee for Standardization, Brussels.

Fardis, M. N., and Panagiotakos, T. B. (1997). "Seismic design and response of bare and infilled reinforced concrete buildings – Part II: Infilled structures." *J. Earthquake Eng.*, 1(3), 473-503.

Fardis, M. N. (2000). "Design provisions for masonry-infilled RC frames." *Proc.12th World Conf. Earthq. Engrg.*, Auckland, New Zeland.

Harajli, M., ElKhatib, H., and Tomas San-Jose, J. (2010). "Static and cyclic out-of-plane response of masonry walls strengthened using textile-mortar system." *J. Mater. Civ. Eng.*, 22(11), 1171-1180.

Koutas, L., Pitytzogia, A., Triantafillou, T. C., and Bousias, S. N. (2014). "Strengthening of infilled reinforced concrete frames with textile-reinforced mortar (TRM): Study on the development and testing of textile-based anchors." *J. Comp. Constr.*, doi:10.1061/(ASCE)CC.1943-5614.0000390.

Kyriakides, M. A., and Billington, S. L. (2008). "Seismic retrofit of masonry-infilled non-ductile reinforced concrete frames using sprayable ductile fiber-reinforced cementitious composites." *Proc. 14th World Conf. Earthq. Engrg.,* Beijing, China.

Loreto, G., Leardini, L., Arboleda, D., and Nanni, A. (2014). "Performance of RC slab-type elements strengthened with fabric-reinforced cementitious-matrix composites." *J. Compos. Constr.*, doi: 10.1061/(ASCE)CC.1943-5614.0000415.

Mehrabi, A. B., Shing P. B., Schuller, M. P., and Noland, J. L. (1996). "Experimental evaluation of masonry-infilled RC frames." *J. Struct. Eng.*, 122(3), 228-237.

Ozcebe, G., Ersoy, U., Tankut, T., Erduran, E., Keskin, O., and Mertol. C. (2003). "Strengthening of brick-infilled RC frames with CFRP." *TUBITAK Structural Engineering Research Unit Report No. 2003-1*, METU, Ankara, Turkey.

Ozden, S., Akguzel, U., and Ozturan T. (2011). "Seismic strengthening of infilled reinforced concrete frames with composite materials." *ACI Struct. J.*, 108(4), 414-422.

Papanicolaou, C. G., Triantafillou, T. C., Karlos, K., and Papathanasiou, M. (2007). "Textile-reinforced mortar (TRM) versus FRP as strengthening material of URM walls: in-plane cyclic loading." *Mater. Struct.*, 40(10), 1081-1097.

Papanicolaou, C. G., Triantafillou, T. C., Papathanasiou, M., and Karlos, K. (2008). "Textile-reinforced mortar (TRM) versus FRP as strengthening material of URM walls: out-of-plane cyclic loading." *Mater. Struct.*, 41(1), 143-157.

Papanicolaou, C. G., Triantafillou, T.C., and Lekka, M. (2011). "Externally bonded grids as strengthening and seismic retrofitting materials of masonry panels." *Constr. Build. Mater.,* 25(2), 505-514.

Prota, A., Marcari, G., Fabbrocino, G., Manfredi, G., and Aldea, C. (2006). "Experimental in-plane behavior of tuff masonry strengthened with cementitious matrix–grid composites." *J. Compos. Constr.*, 10(3), 223–233.

Saatcioglu, M., Serrato, F., and Foo, S. (2005). "Seismic performance of masonry infill walls retrofitted with CFRP sheets." *SP-230: 7th International Symposium on Fiber-Reinforced (FRP) Polymer Reinforcement for Concrete Structures,* Paper 20, 341-354, Shield C., Busel J., Walkup S., Gremel D., (eds.), American Concrete Institute, Farmington Hills.

Triantafillou, T. C., Papanicolaou, C. G., Zisimopoulos, P., and Laourdekis, T. (2006). "Concrete confinement with textile reinforced mortar (TRM) jackets", *ACI Struct. J.*, 103(1), 28-37.

Triantafillou, T. C., and Papanicolaou, C. G. (2006). "Shear strengthening of RC members with textile reinforced mortar (TRM) jackets", *Mater. Struct.*, 39(1), 85-93.

Yuksel, E., Ilki, A., Erol, G., Demir, C., and Karadogan, H. F. (2006). "Seismic retrofitting of infilled reinforced concrete frames with CFRP composites." Advances in earthquake engineering for urban risk reduction, 285-300, Wasti T., Ozcebe G., (eds.), Springer, Dordrecht.

List of Figures

Table 1. Properties of Textiles

Property	Uncoated carbon fibers	Polymer-coated E-glass fibers	Uncoated basalt fibers (used in anchors)
Mesh size (mid-roving to mid-roving grid spacing)	10x10 mm	25x25 mm	25x25 mm
Net grid spacing	7 mm	21 mm	23 mm
Weight	348 g/m^2	405 g/m^2	192 g/m^2
Tensile strength per running meter	157 kN/m*	115 kN/m**	66 kN/m**
Rupture strain	1.5 %	2.5 %	3.15 %
Modulus of elasticity	225 GPa	73 GPa	89 GPa
Fiber density	1.8 g/cm^3	2.6 g/cm^3	2.66 g/cm^3

* Calculated using nominal value of thickness (obtained from the equivalent smeared distribution of fibers); **taken from data sheets of the manufacturer.

Figures

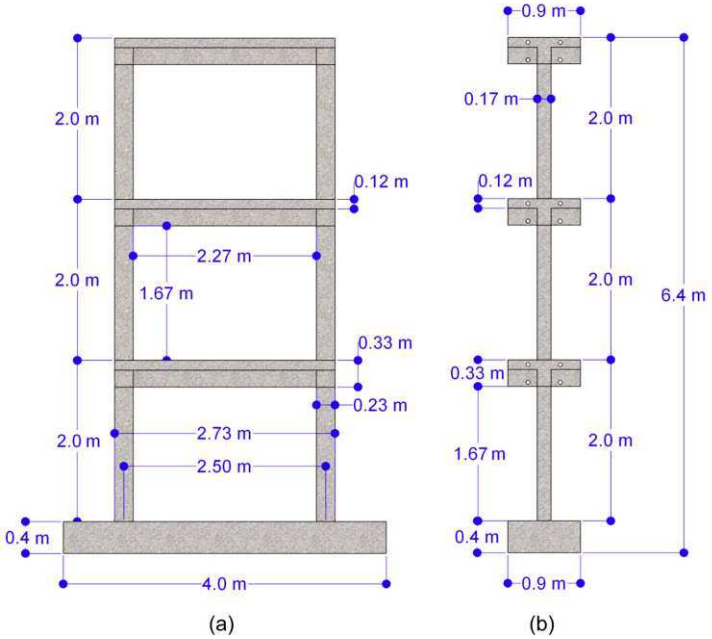

Fig. 1

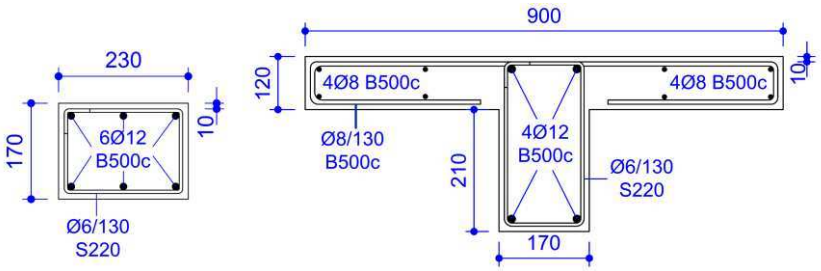

Fig. 2

Fig. 3

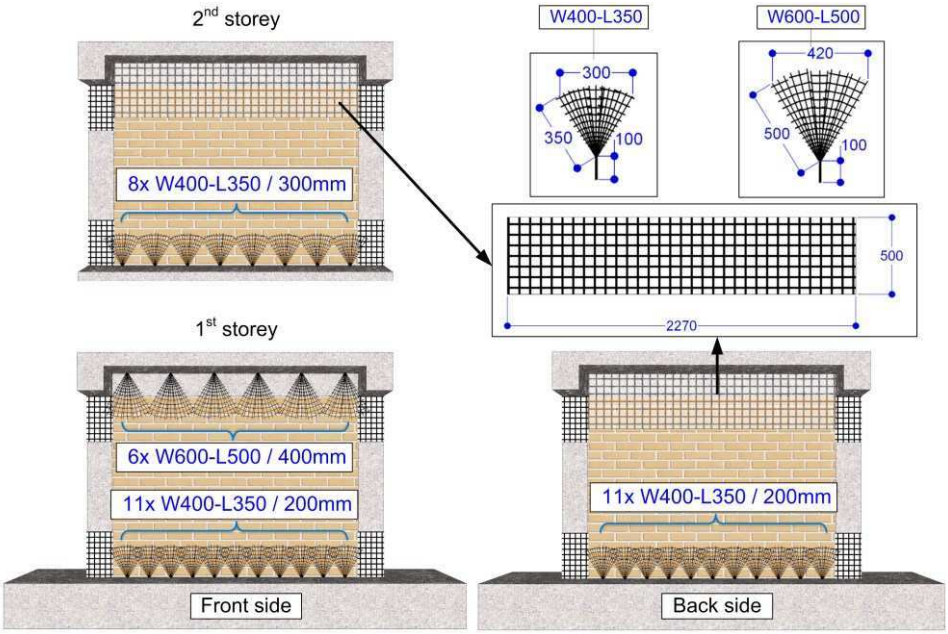

Fig. 4

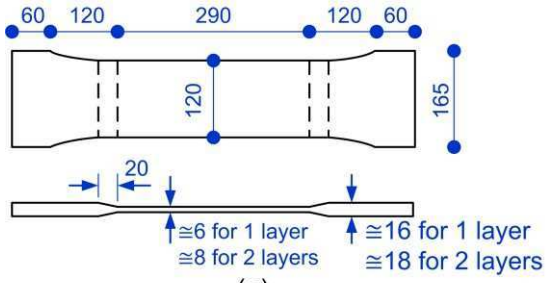

(a)

(b) (c)

Fig. 5

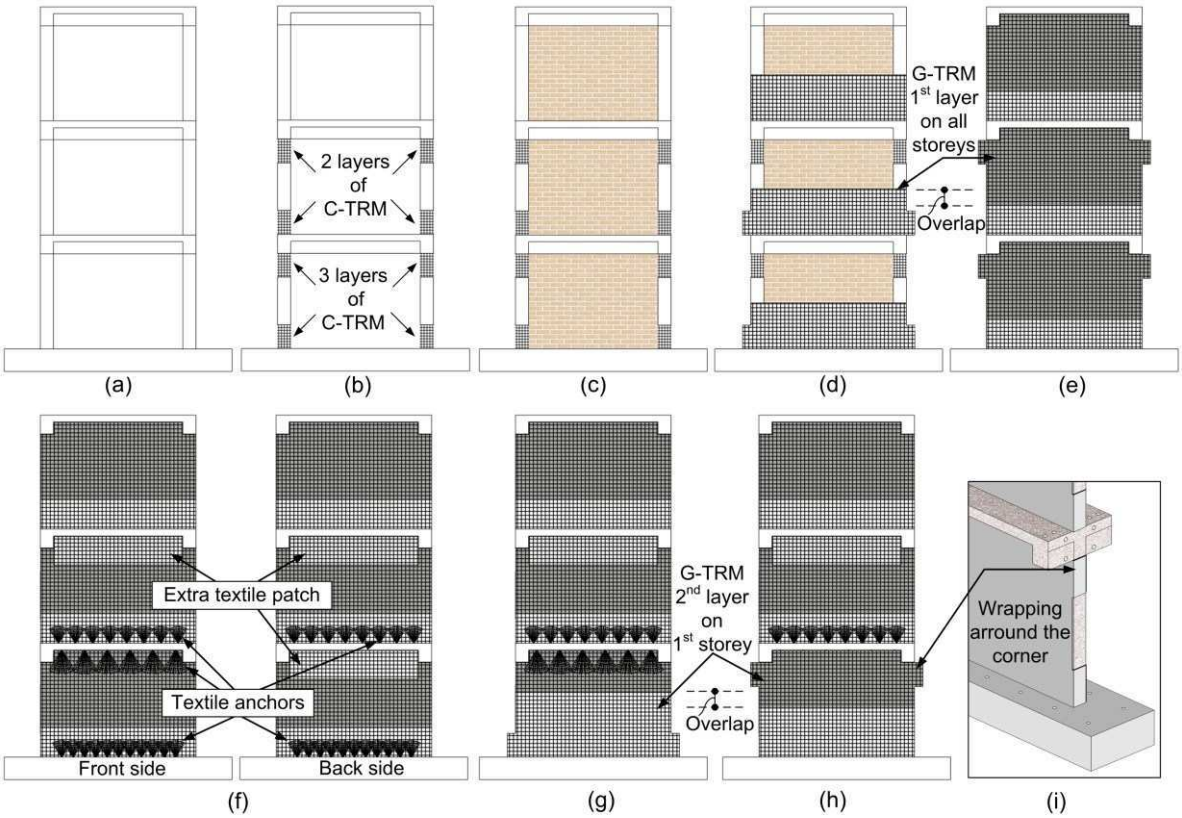

Fig. 6

Fig. 7

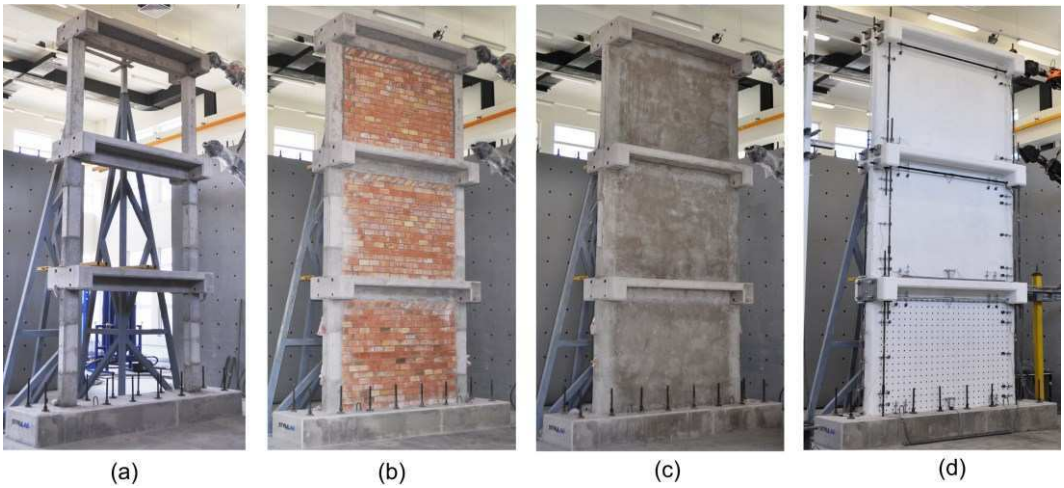

Fig. 8

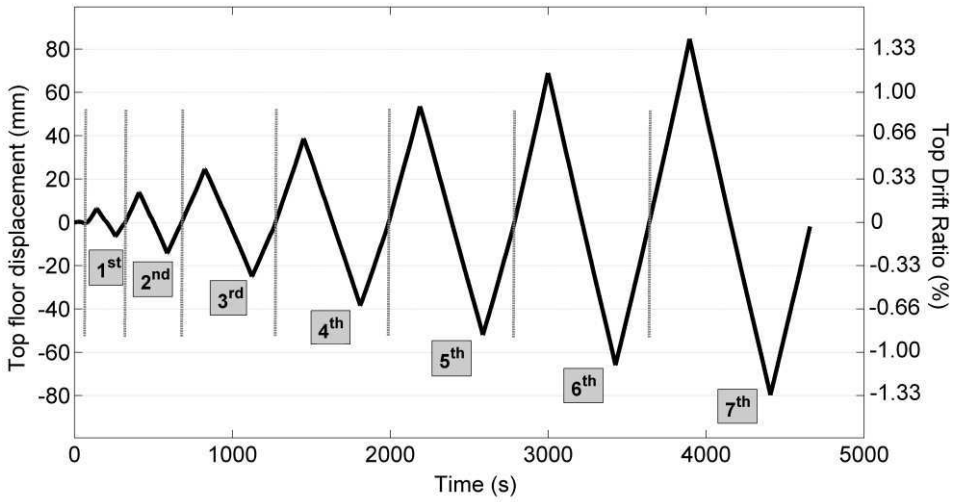
Top floor displacement (mm)
Top Drift Ratio (%)
Time (s)
1st
2nd
3rd
4th
5th
6th
7th

Fig. 9

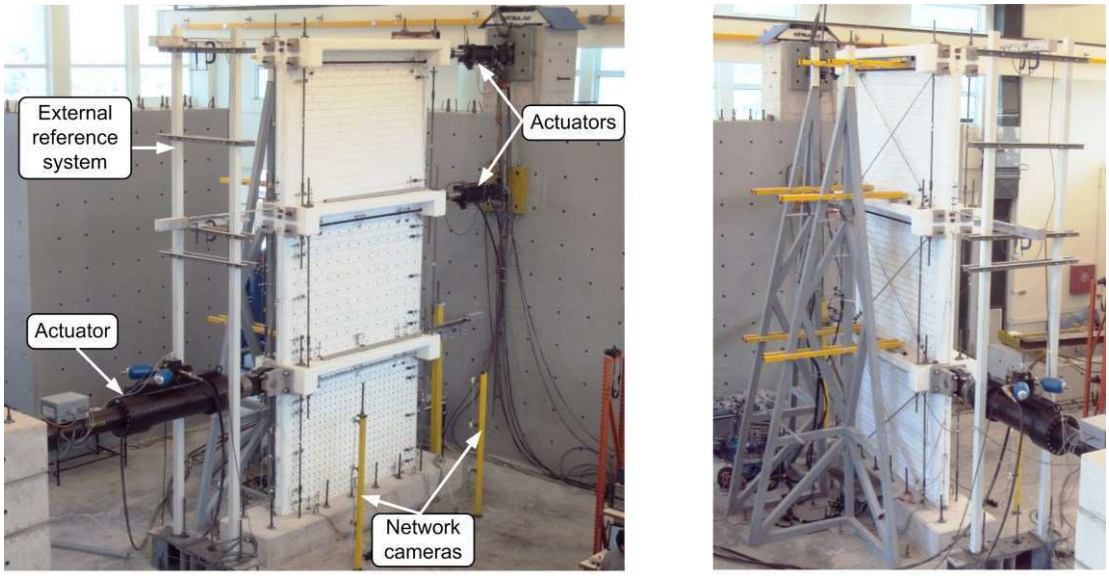
External reference system
Actuators
Actuator
Network cameras
(a)
(b)

Fig. 10

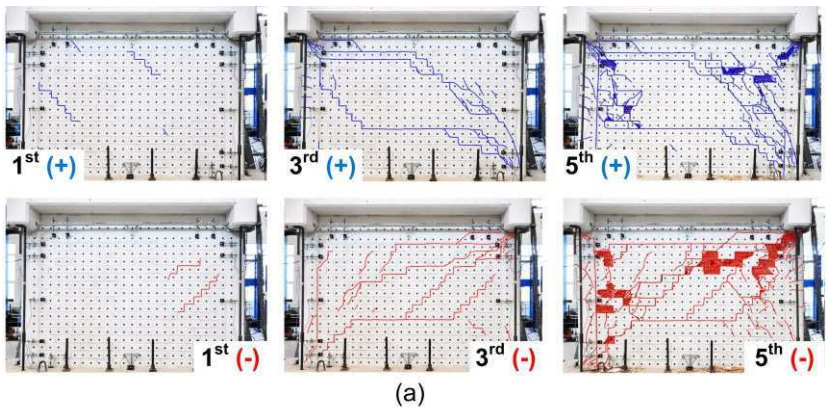

(a)

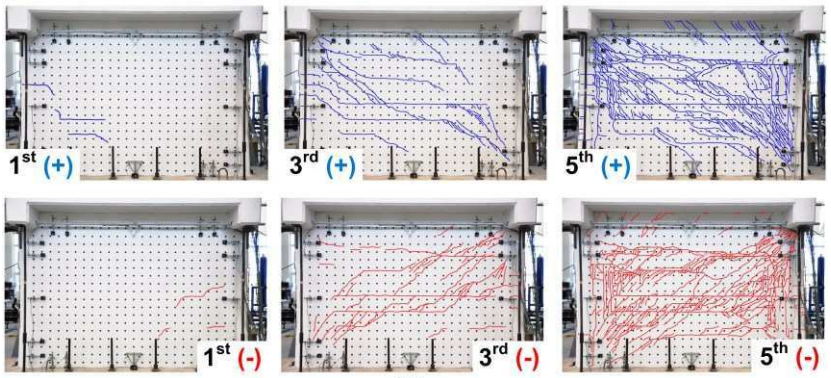

(b)

Fig. 11

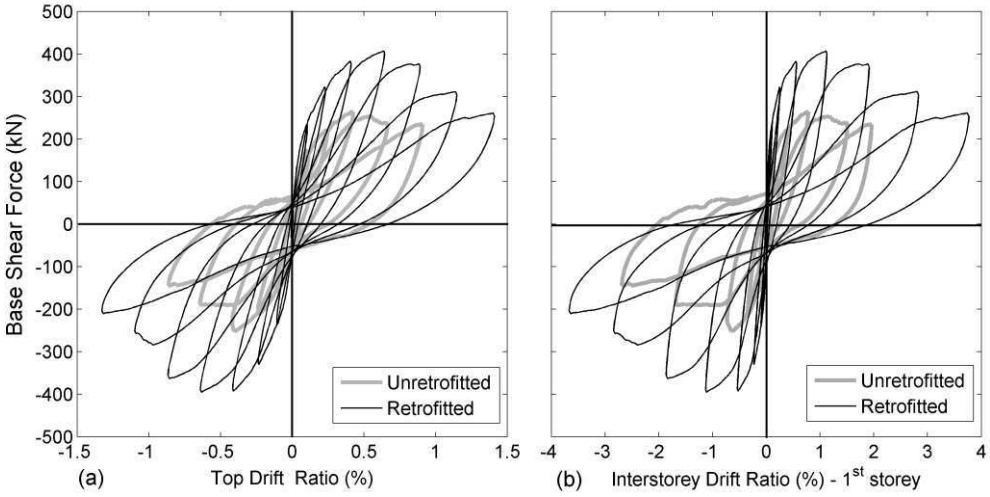

Fig. 12

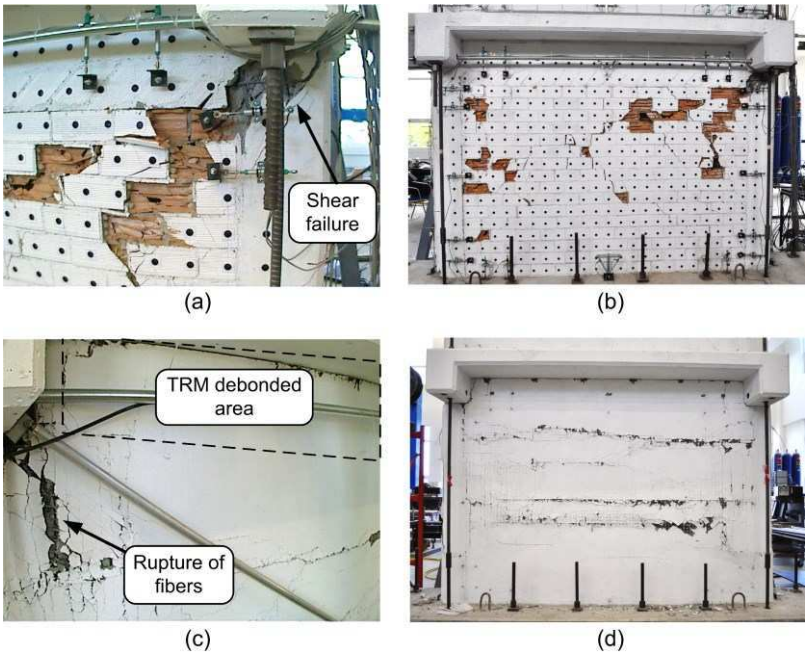

Fig. 13

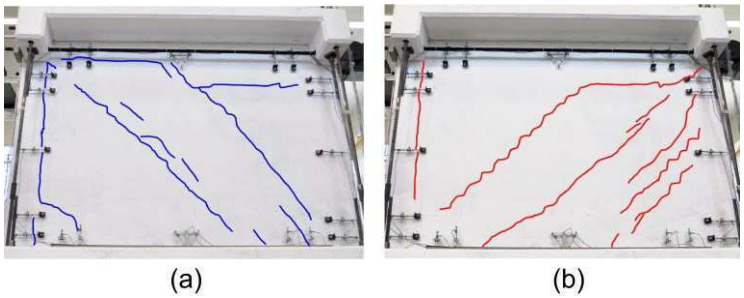

Fig. 14

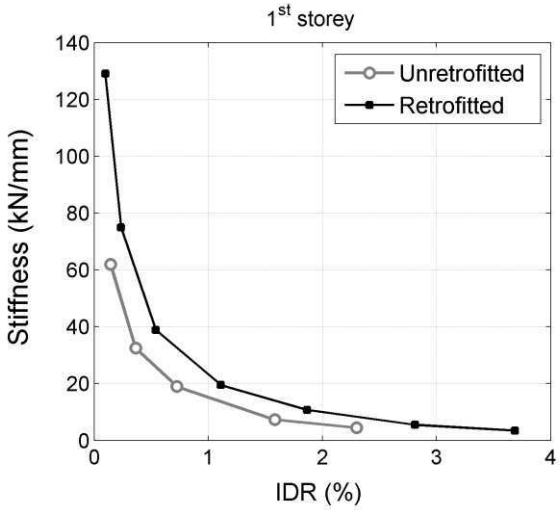

Fig. 15

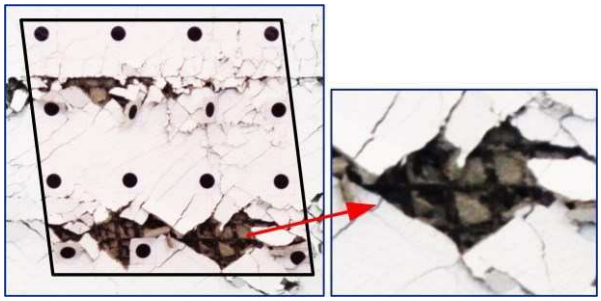

Fig. 16

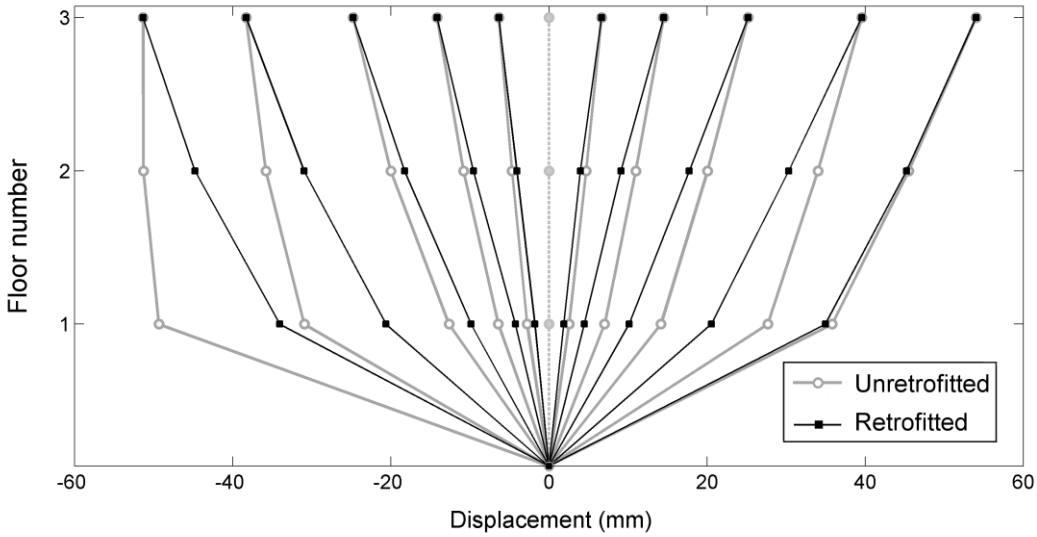

Fig. 17

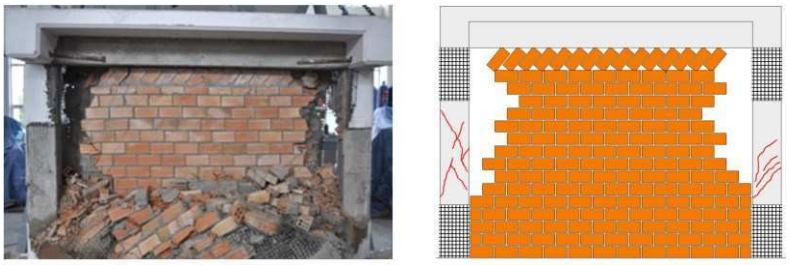

Fig. 18